27-8-2007

Optimal Adaptive Hyperbolic Companding for OFDM

Darryn Lowe
University of Wollongong, darrynl@uow.edu.au

Xiaojing Huang
University of Wollongong, huang@uow.edu.au

Optimal Adaptive Hyperbolic Companding for OFDM

Abstract

In this paper, we derive and analyze a companding algorithm based on the hyperbolic tangent and inverse hyperbolic tangent functions for use in orthogonal frequency division multiplexing (OFDM) transceivers. Probability density functions (PDFs) that approximate the transmitted and received OFDM signals in the presence of additive white Gaussian noise (AWGN) are derived and used to analyze the degree of companding relative to the signal-to-noise ratio (SNR) and clipping level. A set of optimal companding linearity coefficients for the multiband OFDM (MB-OFDM) ultra-wideband (UWB) standard are presented.

Disciplines

Physical Sciences and Mathematics

Publication Details

This conference paper was originally published as Lowe, D, Huang, X, Optimal Adaptive Hyperbolic Companding for OFDM, 2nd International Conference on Wireless Broadband and Ultra Wideband Communications AusWireless 2007, 27-30 Aug, 24-24.

Optimal Adaptive Hyperbolic Companding for OFDM

Darryn Lowe and Xiaojing Huang
School of Electrical, Computer and Telecommunications Engineering
University of Wollongong
Wollongong, Australia, 2522
Email: {darrynl, huang}@uow.edu.au

***Abstract*— In this paper, we derive and analyze a companding algorithm based on the hyperbolic tangent and inverse hyperbolic tangent functions for use in orthogonal frequency division multiplexing (OFDM) transceivers. Probability density functions (PDFs) that approximate the transmitted and received OFDM signals in the presence of additive white Gaussian noise (AWGN) are derived and used to analyze the degree of companding relative to the signal-to-noise ratio (SNR) and clipping level. A set of optimal companding linearity coefficients for the multi-band OFDM (MB-OFDM) ultra-wideband (UWB) standard are presented.**

I. Introduction

Orthogonal frequency division multiplexing (OFDM) has several advantages over single-carrier modulations [1]. These include robustness against multipath interference, low complexity equalization and a power spectrum that can be adjusted to avoid interferers. Unfortunately, since OFDM uses a plurality of subcarriers, the cost of obtaining these features is a significant increase to the signal's peak-to-average power ratio (PAPR) [2].

Given the popularity of OFDM systems, many techniques have been proposed to mitigate the PAPR problem. Generally, these can be classified depending on their use of explicit side channel information. For example, the insertion of dummy sequences prior to the inverse fast fourier transform (IFFT) [3] requires no receiver modifications. Other techniques, such as using block codes to create a pool of candidate transmissions [4] from which the signal with the lowest PAPR can be selected, requires that the receiver be explicitly informed as to which block code was used. Of all these techniques, the simplest solution is to clip the transmitted signal when either the real or imaginary components exceed some arbitrary value. Unfortunately, this highly non-linear operation can introduce significant distortions that can corrupt the frequency-domain data constellations.

To mitigate the corruption caused by clipping, it is often suggested that companding algorithms [5] be used. In this paper, we propose using the hyperbolic tangent and its inverse, the hyperbolic arctangent, for such a purpose. These functions, in addition to possessing trigonometric identities that make them analytically tractable, also share the property that they are linear for small values. This is desirable since it allows the possibility of legacy support wherein a transmitted signal that has undergone such companding could be processed by a traditional receiver. This approach to companding therefore has the potential to be more practical than previous adaptive companding techniques that are not backwards compatible [6].

In addition to deriving hyperbolic companding functions, we also identify the relationship between the degree of non-linearity and the signal-to-noise ratio (SNR) so as to permit the degree of companding to be adaptive to channel conditions. In other words, we develop a low-complexity technique wherein the optimal linearity coefficients are found given the receiver SNR and clipping level. In other words, since a multi-rate transmitter must estimate the noise strength at the receiver in order to select an appropriate modulation density and forward error correction (FEC), there is a trivial increase to complexity in using this same information to tune the degree of companding.

Although the hyperbolic tangent has previously been presented as a companding algorithm [7], this paper extends previous work by considering the probability density function (PDF) of the inverse hyperbolic tangent function as well as deriving a relationship between companding linearity, signal strength, noise power and clipping levels.

This paper is organized as follows. In Section II we begin our analysis by defining the signal model and deriving a simplified PDF that models a complex-valued OFDM transmission. This is followed by the companding analysis of Section III that defines the hyperbolic tangent and arctangent functions and derives PDFs for both the transmitted and received signals. The expected noise power at the input to the receiver baseband is then parameterized such that the numerical analysis in Section IV can identify the optimal non-linearity coefficients for the multi-band OFDM (MB-OFDM) ultra-wideband (UWB) standard. We conclude with Section V where we summarize our findings and identify future work.

II. Signal Model

An OFDM transmitter transforms a set of N frequency-domain symbols, often modulated using techniques such as quadrature phase shift keying (QPSK), into N complex time-domain samples. Assuming that each of the N subcarriers are independent, the law of large numbers mandates that the real and imaginary components of $\mathbf{t}$ will approach a Gaussian distribution. In other words, the absolute value of the transmitted signal samples will posses a Rayleigh distribution.

The 2nd International Conference on Wireless
Broadband and Ultra Wideband Communications (AusWireless 2007)
0-7695-2842-2/07 $25.00 © 2007 IEEE

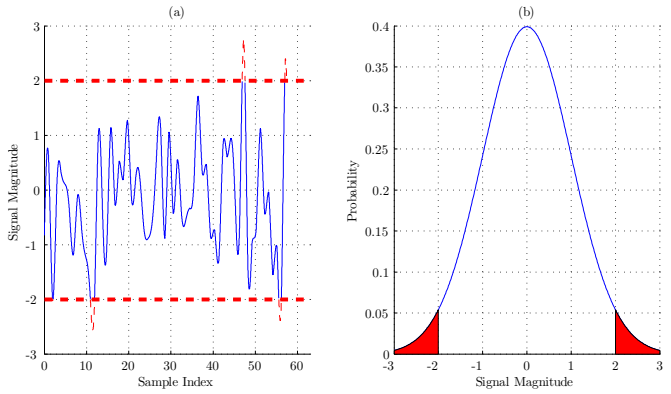

Fig. 1. Example of clipping on the real portion of a Gaussian distributed OFDM signal shown (a) in time-domain and (b) as a probability distribution.

Since the PAPR of an OFDM signal is directly proportional to N, it is almost inevitable that a practical baseband implementation will have to clip the signal. For example, with some contemporary OFDM systems using between 128 and 4096 subcarriers, the PAPR of an unmodified OFDM signal would be prohibitively high.

To model an OFDM signal, we denote the PDF of a Gaussian distributed random variable with variance σ^2 and mean μ as

$$P_G(x) = \frac{1}{\sigma\sqrt{2\pi}} \exp\left(-\frac{1}{2}\frac{(x-\mu)^2}{\sigma^2}\right) \tag{1}$$

over the domain $x\epsilon\,(-\infty, \infty)$. Note that we do not use a Rayleigh distribution since we assume that the in-phase (I) and quadrature (Q) components of the signal will be processed independently.

Since an OFDM signal is complex-valued and zero-mean, i.e. $\mu = 0$, we can denote the normalized expected error due to clipping values that exceed an arbitrary cutoff $L > 0$ as

$$E^2_{\text{clip}} = \frac{1}{2\sigma^2}\int_{-\infty}^{\infty}\int_{-\infty}^{\infty} P_G(x)P_G(y)\left[g(x)^2 + g(y)^2\right] dxdy \tag{2}$$

where $g(x)$ is the error due to a given degree of clipping and can be denoted

$$g(x) = \begin{cases} |x| - L & \text{if } |x| > L, \\ 0 & \text{otherwise.} \end{cases} \tag{3}$$

An example of how clipping impacts a signal with a Gaussian distribution is shown in Fig. 1 where, with $\sigma = 1$ and $L = 2$, it can be observed that the signal peaks are truncated.

Assuming that the real and imaginary components of an OFDM signal are independent, we can simplify (2) by focusing only on a real-valued zero-mean Gaussian distribution. In other words, we can denote the expected clipping error as

$$E^2_{\text{clip}} \approx \frac{1}{\sigma^2}\int_{-\infty}^{\infty} P_G(x)g(x)^2 dx \tag{4}$$

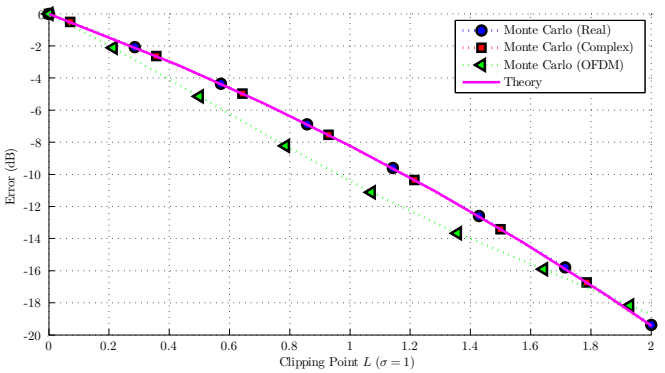

Fig. 2. Error introduced by clipping level.

Since the clipping causes no error when $|x| <= L$, as depicted in the highlighted region of Fig. 1b, we can further simplify (4) by changing the limits on the integration to yield

$$E^2_{\text{clip}} \approx \frac{2}{\sigma^2}\int_{-\infty}^{-L} P_G(x)\,(L+x)^2\,dx \tag{5}$$

and then solving for

$$E^2_{\text{clip}} = \left(1 + \frac{L^2}{\sigma^2}\right)\left[1 - \text{erf}\left(\frac{L}{\sigma\sqrt{2}}\right)\right] - \frac{L\sigma\sqrt{2}}{\sqrt{\pi}}\exp\left(-\frac{L^2}{2\sigma^2}\right). \tag{6}$$

Comparisons of (2) and (6) to Monte Carlo simulations of an OFDM signal are provided in Fig. 2. With the Monte Carlo OFDM model based on MB-OFDM, with 128 random QPSK subcarriers per symbol, we can conclude that (6) is an approximate upper-bound on clipping error. In other words, we observe that we can evaluate the performance of the companding techniques developed in the following section using a real-valued zero-mean Gaussian signal model without significant loss of accuracy.

III. Companding

We propose the use of the hyperbolic tangent function [8]

$$\tanh x \equiv \frac{\sinh x}{\cosh x} = \frac{e^{2x} - 1}{e^{2x} + 1} \tag{7}$$

to reduce the magnitude of the OFDM signal peaks at the transmitter. We will then use the inverse hyperbolic tangent function

$$\tanh^{-1} x \equiv \text{atanh}\, x = \frac{1}{2}\left[\ln(1+x) - \ln(1-x)\right]. \tag{8}$$

at the receiver to recover the original signal. Note that since the inverse hyperbolic tangent is only real when $x < 1$, we can simplify the receiver expression to

$$\tanh^{-1} x = \frac{1}{2}\ln\frac{1+x}{1-x}. \tag{9}$$

In order to control the degree of companding, we introduce a linearity coefficient $C > 0$ to (7) and (9) to yield

$$C\tanh\left(\frac{x}{C}\right) \tag{10}$$

The 2nd International Conference on Wireless
Broadband and Ultra Wideband Communications (AusWireless 2007)
0-7695-2842-2/07 $25.00 © 2007 IEEE

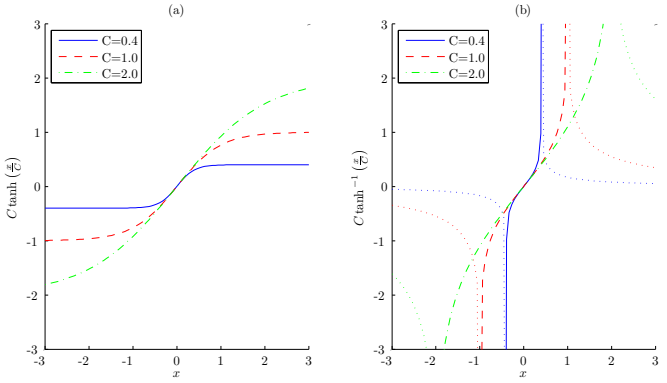

Fig. 3. Example of functions (a) $C\tanh\left(\frac{x}{C}\right)$ and (b) $C\,\text{atanh}\left(\frac{x}{C}\right)$.

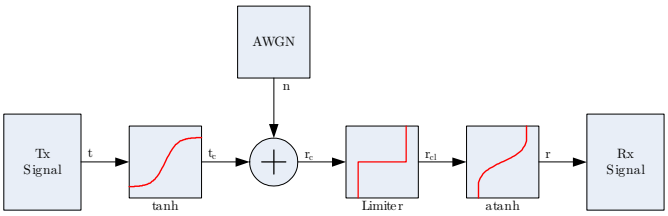

Fig. 4. Block diagram of companding.

and

$$C\,\text{atanh}\left(\frac{x}{C}\right) \tag{11}$$

respectively. An example of the impact of C is shown in Fig. 3, with the non-real region of the inverse hyperbolic tangent denoted with a dotted line. This figure aids in making two key observations concerning the impact of C. Firstly, with

$$\lim_{C\to 0} C\tanh\frac{x}{C} = C\,\text{sgn}\,x, \tag{12}$$

we observe that small values of C will cause very aggressive non-linear companding. Secondly, with

$$\lim_{C\to\infty} C\tanh\frac{x}{C} = \lim_{C\to\infty} C\,\text{atanh}\frac{x}{C} = x, \tag{13}$$

we observe that large values of C will produce an almost perfectly linear response and thereby effectively disable the companding.

A block diagram depicting the application of the companding algorithm is shown in Fig. 4. As per our previous simplification wherein we decided to model the OFDM signal and corrupting AWGN as real-valued zero-mean Gaussian noise, we can denote the PDF of the random variables t and n as per (1) with variances of σ_T^2 and σ_N^2 respectively.

A. Transmitter

Let z be a Gaussian distributed random variable with mean $\mu = 0$ and variance σ^2 such that $P_z(x)$ is equivalent to (1). In the context of Fig. 4, we will be using z to model the Gaussian distributed OFDM signal t.

Assuming that $f_n(x)$ is an arbitrary real-valued function in the region $x\epsilon(-\infty,\infty)$, we can denote the PDF of $f_n(z)$ as

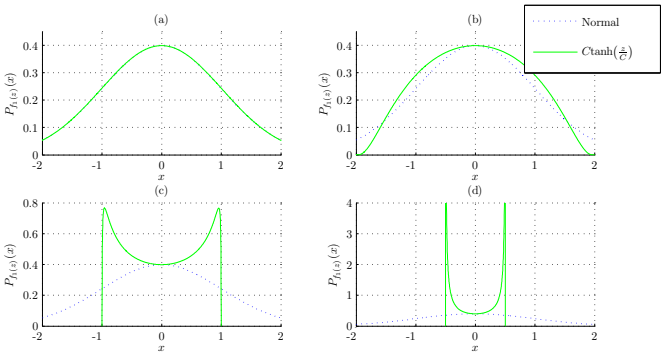

Fig. 5. Example PDFs for $f_1(z)$ with $\mu = 0$, $\sigma^2 = 1$ and (a) $C = 10$, (b) $C = 2$, (c) $C = 1$ and (d) $C = 0.5$

[8]

$$P_{f_n(z)}(x) = P\left(f_n^{-1}(x)\right)\frac{d}{dx}f_n^{-1}(x) \tag{14}$$

Accordingly, if $f_1(x) = C\tanh\left(\frac{x}{C}\right)$ and $f_1^{-1}(x) = C\,\text{atanh}\left(\frac{x}{C}\right)$, then the identity

$$\frac{d}{dx}f_1^{-1}(x) = \frac{d}{dx}C\,\text{atanh}\left(\frac{x}{C}\right) = \frac{C^2}{C^2 - x^2} \tag{15}$$

can be substituted into (14) to yield

$$P_{f_1(z)}(x) = \begin{cases} 0 & \text{if } x < -C, \\ \dfrac{C^2\exp -\frac{1}{2}\frac{C^2\,\text{atanh}\left(\frac{x}{C}\right)^2}{\sigma^2}}{\sigma\left(C^2 - x^2\right)\sqrt{2\pi}} & \text{if } -C \le x \le C, \\ 0 & \text{if } x > C. \end{cases} \tag{16}$$

where the piecewise function is needed since $f_1^{-1}(x)$ is only real for $-C \le x \le C$. Fortunately, since $f_1^{-1}(x)$ is asymptotic in terms of C, i.e. $\lim_{|x|\to C} f_1^{-1}(x) = 0$, the discontinuity has no impact on the PDF.

Several examples of the transmitted signal distribution are shown in Fig. 5 where it can observed that the degree of companding is inversely proportional to C. In other words, a low value of C will result in a greatly reduced PAPR.

We therefore conclude that the hyperbolic companded time-domain OFDM signal

$$t_c = C\tanh\frac{t}{C}, \tag{17}$$

will have the PDF of (16) where $\sigma^2 = \sigma_T^2$.

B. Peak to Average Power

An OFDM signal will generally be clipped to reduce the PAPR, often due to the limited dynamic range of practical hardware. As suggested by comparing the PDFs of Fig. 5, hyperbolic companding will reduce the PAPR more than clipping as per (3) when $L = C$.

To quantify the difference, we can use denote the variance of the zero-mean companded transmitted signal as

$$\sigma_{t_c}^2 = \int_{-\infty}^{\infty} P_{f_1(z)}(x)x^2dx. \tag{18}$$

The 2nd International Conference on Wireless
Broadband and Ultra Wideband Communications (AusWireless 2007)
0-7695-2842-2/07 $25.00 © 2007 IEEE

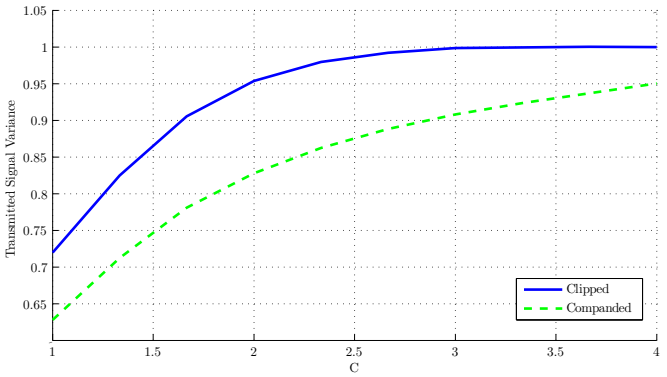

Fig. 6. Comparison of transmitted signal variance for companding vs. clipping.

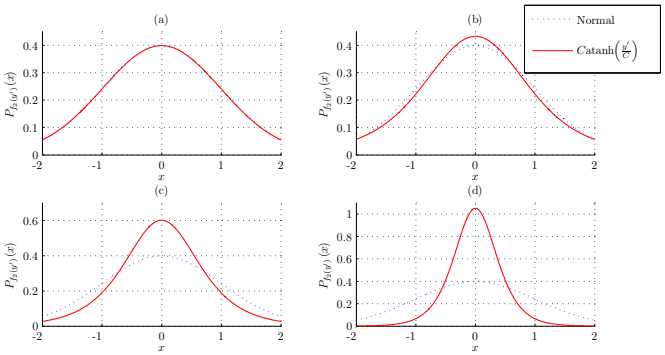

Fig. 7. Example PDFs for $f_2(y)$ with $\mu = 0$, $\sigma^2 = 1$ and (a) $C = 10$, (b) $C = 2$, (c) $C = 1$ and (d) $C = 0.5$

with Fig. 6 showing a comparison for a range of C when $\sigma_T^2 = 1$. It can be observed that the companded signal has slightly lower variance than the original signal. This is to be expected since the hyperbolic tangent has no discontinuities.

C. Receiver

To consider the effect of the inverse hyperbolic tangent on the AWGN-corrupted signal at the receiver, the PDF of the received signal r_c can be derived using similar logic as used for the transmitter. To that end, we define y as a Gaussian distributed random variable as per (1), with variance $\sigma^2 = \sigma_N^2$ and mean $\mu = t_c$.

If we define $f_2(x) = C\,\text{atanh}\left(\frac{x}{C}\right)$ and $f_2^{-1}(x) = C\tanh\left(\frac{x}{C}\right)$, then (14) can be solved by substituting the identity

$$\frac{d}{dx} f_2^{-1}(x) = \frac{d}{dx} C\tanh\left(\frac{x}{C}\right) = 1 - \tanh\left(\frac{x}{C}\right)^2. \quad (19)$$

However, before we can perform this substitution, we must first restrict the range of y so that $f_2(y)$ is real. In other words, if we denote y' as

$$y' = \begin{cases} -L & \text{if } y < -L, \\ y & \text{if } -L \le y \le L, \\ L & \text{if } y > L, \end{cases} \quad (20)$$

with $L < C$ to keep $f_2(x)$ real, then we are effectively using the limiter of Fig. 4 to limit the noise that would otherwise cause the received signal to exceed the transmitter's maximum amplitude of C. As a result, the PDF of y' will have discontinuities at $\pm L$. Furthermore, it is worth nothing that since the limiter will be realized via the finite dynamic range of the digital-to-analogue converter, it incurs no hardware complexity.

We can denote the impact of the limiter on the PDF of $f_2(y')$ as a scaling such that

$$\int_{-\infty}^{\infty} P_{f_2(y')}(x)dx + \alpha = 1 \quad (21)$$

where

$$\begin{aligned} \alpha &= \alpha_{\text{lower}} + \alpha_{\text{upper}} \\ &= \int_{-\infty}^{-L} P_y(x)dx + \int_{L}^{\infty} P_y(x)dx \\ &= \frac{1}{2}\,\text{erf}\left(\frac{\mu + L}{\sigma\sqrt{2}}\right) + \frac{1}{2}\,\text{erf}\left(\frac{\mu - L}{\sigma\sqrt{2}}\right) \end{aligned} \quad (22)$$

is obtained using the CDF for a Gaussian distributed random variable.

Finally, by substituting (19) into (14), the PDF of $f_2(y')$ can be denoted as

$$P_{f_2(y')}(x) = \frac{\exp -\frac{1}{2}\frac{\left(C\,\text{atanh}\left(\frac{x}{C}\right)-\mu\right)^2}{\sigma^2}\left(1 - \tanh\left(\frac{t}{C}\right)^2\right)}{\sigma\sqrt{2\pi}} \quad (23)$$

with several examples of the received noise distribution shown in Fig. 7.

D. Expected Receiver Error

We can denote the expected error at the receiver when the transmitted signal t_c is known by using the PDF of (21) to denote

$$\begin{aligned} E^2(t_c) = \alpha_{\text{lower}} e^2_{\text{lower}} + \alpha_{\text{upper}} e^2_{\text{upper}} \\ + \int_{-f_2(L)}^{f_2(L)} P_{f_2(y'|_{\mu=t_c})}(x) e^2_{\text{middle}}(x)dx \end{aligned} \quad (24)$$

where e^2_{lower} is the error due to the transmitted signal exceeding the lower cutoff $-L$ and can be denoted

$$e^2_{\text{lower}} = [f_2(L) + f_2(t_c)]^2 \quad (25)$$

and e^2_{upper} is the error due to the transmitted signal exceeding the upper cutoff L and can be denoted

$$e^2_{\text{upper}} = [f_2(L) - f_2(t_c)]^2 \quad (26)$$

and $e^2_{\text{middle}}(x)$ is the difference between the noise x and the transmitted signal and can be denoted

$$e^2_{\text{middle}}(x) = [x - f_2(t_c)]^2. \quad (27)$$

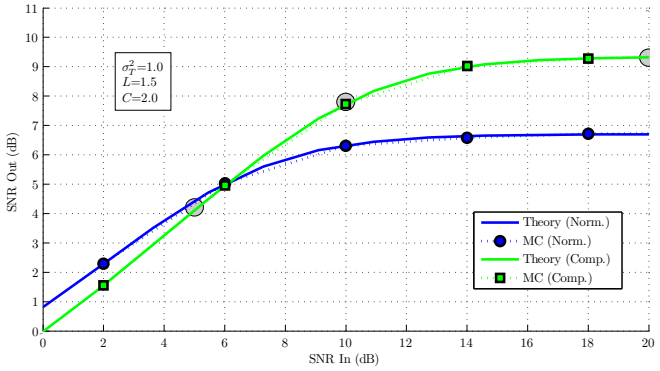

Fig. 8. Comparison of theoretical and Monte Carlo approaches to analyzing companding with hyperbolic tangents.

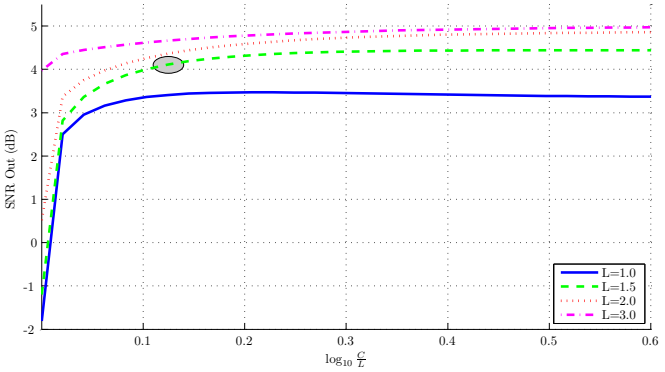

Fig. 9. SNR relative to degree of companding when SNR is 5 dB.

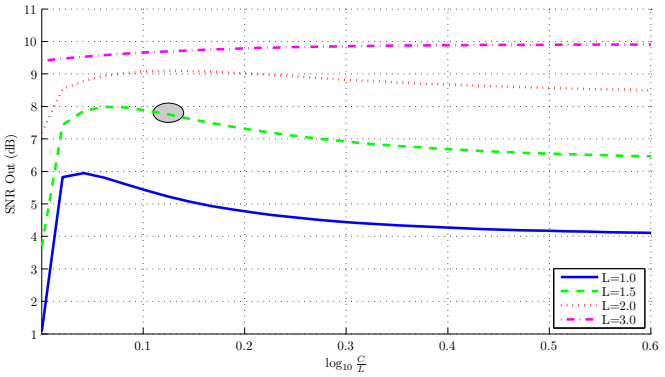

Fig. 10. SNR relative to degree of companding when SNR is 10 dB.

Since the PDF of the transmitted signal is given by (16), we can use (24) to denote the overall expected error at the receiver due to AWGN as

$$E^2_{\text{companded}} = \int_{-L}^{L} P_{f_1(z)}(s)E^2(s)ds \tag{28}$$

The accuracy of this signal model is demonstrated in Fig. 8, which is calculated via application of numeric trapezoidal integration to 28, and shows the input and output SNRs for an OFDM transmitter with transmit energy $\sigma_T^2 = 1$, clipping limit $L = 1.5$ and linearity coefficient $C = 2$. The three highlighted regions correspond to the regions in Fig. 9, 10 and 11 where alternate companding and clipping coefficients are considered.

Note observe that Fig. 8 denotes a system subjected to such aggressive clipping, with $L = 1.5\sigma_T^2$, which means that the effective receiver SNR can never exceed 6.5 dB when no companding is used. In other words, at high SNR, the clipping causes so much distortion that it dominates over the impact of AWGN and imposes a hard limit on performance. This would that only low data rates could be supported. Fortunately, by applying companding at a degree of $C = 2$, we can improve the maximum effective SNR by up to 2.5 dB. Further, as per our original speculation that the optimal degree of companding is a function of the SNR, we observe that increasing the degree of companding to $C = 2$ actually degrades performance.

In the following section, we will examine different values of C, as functions of L and the SNR, in order to identify the optimal degree of companding for different applications.

IV. Results

The performance of hyperbolic companding is dependant on four factors, namely the signal energy σ_T^2, the noise energy σ_N^2, the clipping level L and the linearity coefficient C. In this section, we use numeric integration to quantify the relationship between the linearity coefficient and the other parameters. This model is then used to identify the optimal linearity coefficients for each of the data rates in the MB-OFDM UWB standard.

A. SNR vs. Linearity Coefficients

In using (28) to model the relationship between SNR and the linearity coefficient C, we consider three SNRs at 5 dB, 10 dB and 20 dB. In each case, note that the horizontal axis shows the linearity coefficient as $\log_{10}\frac{C}{L}$ since the exact value of the coefficient is more significant when it is small. Further, to facilitate comparison with Fig. 10, the denoting an equivalent C and L is highlighted.

Fig. 9 shows the high-noise scenario where the SNR is only 5 dB. We observe that overly aggressive companding can easily render the system almost useless, particularly when the limiting threshold L is low. This is to be expected given that such companding is further reducing the signal amplitude and thereby exacerbating the impact of the AWGN. Accordingly, we conclude that very low SNRs are best served by effectively disabling the companding entirely.

Fig. 10 reduces the impact of noise by raising the SNR to 10 dB. It can be observed that the increase in SNR has uniformly lowered the optimal linearity coefficients. We note that when the limiting is aggressive, such as $L = 1.5$, even a little companding offers massive improvements in effective SNR.

Fig. 11 shows an extremely low noise scenario with the SNR at 20 dB. In this case, with the effects of noise relatively marginal, it is apparent that the best performance is achieved by aggressively companding the transmitted signal with $C \approx L$ in most cases. The only exception to this is very aggressive transmitter clipping at $L = 1$, where it can be seen that marginal companding offers very slight gains.

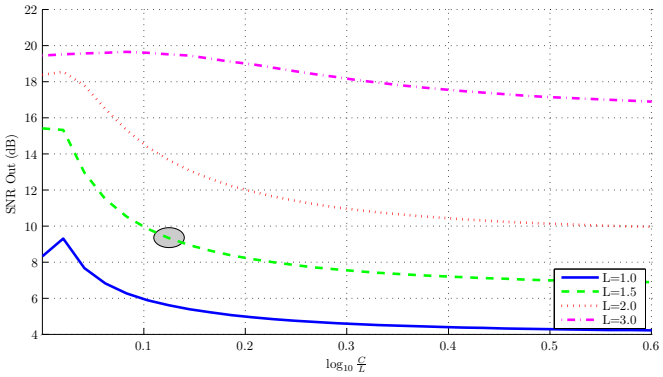

Fig. 11. SNR relative to degree of companding when SNR is 20 dB.

In general, we conclude that the results confirm our intuitive belief that the importance of the linearity coefficient C decreases as the degree of clipping does. In other words, when the transmitter clipping threshold L is high, it is largely inconsequential as how much companding is applied since most signal amplitudes will be well within the linear region regardless. However, when the transmitter clips aggressively, companding can offer several dB of improvement in effective SNR at the receiver.

B. Optimal Linearity Coefficients

MB-OFDM [9] is the first ultra-wideband standard. In addition to providing a range of data rates, from 53.3 Mbps to 480 Mbps, we select MB-OFDM as an example since the short range of the wireless UWB channel incurs delay spreads much less than those associated with other OFDM technologies such as digital television and wireless local area networks (WLANs). This is ideal since this paper does not consider the impact of multipath scatterers [10]; this is an area for future work.

To find the optimal linearity coefficient for a given signal energy σ_T^2, noise energy σ_N^2 and clipping level L, we again solved (28) via numeric integration and used the Simplex search algorithm to find which C resulted in the minimum noise variance at the input to the receiver baseband.

Table I shows the results of the search for each of the data rates and minimum SNR specified by the MB-OFDM standard. Note that the signal energy is normalized such that $\sigma_T^2 = 1$, with the noise power is calculated relative to the minimum receiver sensitivity required by the conformance testing section of the MB-OFDM standard. Also note that the linearity coefficient C is expressed as a multiple of L in a similar way as used for the figures, with the blank cells indicating that the optimal linearity coefficient is so large as to be effectively infinite. This is consistent with the results shown in Fig. 9.

Data Rate (Mbps)	Min. SNR (dB)	$\frac{C}{L}$			
		$L=1$	$L=2$	$L=3$	$L=4$
53.3	5.97	1.36			
80	7.87	1.17			
106.7	8.97	1.12	4.24		
160	10.87	1.07	1.26		
200	12.27	1.05	1.18	2.26	
320	13.97	1.03	1.12	1.61	
400	15.27	1.02	1.09	1.60	2.80
480	16.37	1.02	1.06	1.41	2.00

TABLE I
OPTIMAL LINEARITY COEFFICIENT C.

V. CONCLUSIONS

In this paper, we have derived PDFs for transmitted and received OFDM signals undergoing companding via the hyperbolic tangent and inverse hyperbolic tangent functions. The expected noise variance at the input to the receiver baseband has been calculated. Several examples of the relationship between SNR, clipping level and non-linearity coefficient were given, with optimal non-linearity coefficients identified for all of the data rates in the MB-OFDM UWB standard.

Future work will compare the hyperbolic tangent technique proposed here to other companding algorithms. Future work will also quantify legacy compatibility, the impact of multipath channels and the effects of quantization. We will also develop Monte Carlo simulations to experimentally verify the theoretical work presented here with packet error rate (PER) analysis.

REFERENCES

[1] Z. Wang and G. B. Giannakis, "Wireless multicarrier communications," *IEEE Signal Processing Magazine*, vol. 17, no. 3, pp. 29–48, 2000.
[2] V. Tarokh and H. Jafarkhani, "On the computation and reduction of the peak-to-average power ratio in multicarrier communications," *IEEE Trans. Comm.*, vol. 48, no. 1, pp. 37–44, Jan. 2000.
[3] H. Ryu, J. Lee, and J. Park, "Dummy sequence insertion (DSI) for PAPR reduction in the OFDM communication system," vol. 50, Feb. 2004.
[4] K. Yang and S. Chang, "Peak to average power control in OFDM using standard arrays of linear block codes," vol. 7, Apr. 2003.
[5] X. Wang, T. T. Tjhung, and C. S. Ng, "Reduction of peak to average power ratio of OFDM system using a companding technique," vol. 25, Sept. 1999.
[6] Y. Guo and J. R. Cavallaro, "Reducing peak-to-average power ratio in OFDM systems by adaptive dynamic range companding," in *Proceedings of the 2002 World Wireless Congress*, Sept. 2002.
[7] M. Godfrey, "The tanh transformation," Information Systems Laboratory, Electrical Eengineering Department, Stanford University, Tech. Rep., 1996.
[8] M. Fisz, *Probability Theory and Mathematical Statistics*. John Wiley and Sons, 1963.
[9] *High Rate Ultra Wideband PHY and MAC Standard*, ECMA International ECMA-368, Dec. 2005.
[10] A. F. Molisch, J. R. Foerester, and M. Pendergrass, "Channel models for ultrawideband personal area networks," *IEEE Wireless Commun. Mag.*, pp. 14–21, Dec. 2003.